In Situ Observation of CO Oxidation on Ag(110) (2×1)-O by Scanning Tunneling Microscopy: Structural Fluctuation and Catalytic Activity

ARTICLE *in* THE JOURNAL OF PHYSICAL CHEMISTRY B · SEPTEMBER 2005

Impact Factor: 3.3 · DOI: 10.1021/jp0512154 · Source: PubMed

4 AUTHORS, INCLUDING:

Noriaki Takagi
The University of Tokyo
99 PUBLICATIONS **1,859** CITATIONS
SEE PROFILE

Yoshi Matsumoto
Kyoto University
135 PUBLICATIONS **1,747** CITATIONS
SEE PROFILE

In Situ Observation of CO Oxidation on Ag(110)(2×1)-O by Scanning Tunneling Microscopy: Structural Fluctuation and Catalytic Activity

Osamu Nakagoe,[†,⊥] Kazuya Watanabe,[†,‡] Noriaki Takagi,[†,‡,§] and Yoshiyasu Matsumoto*[,†,‡]

Department of Photoscience, School of Advanced Sciences, The Graduate University for Advanced Studies (Sokendai), Hayama, Kanagawa, 240-0193, Japan, Institute for Molecular Science, Okazaki, Aichi, 444-8585, Japan, and Department of Advanced Materials Science, University of Tokyo, Kashiwa, Chiba, 277-8561, Japan

Received: March 9, 2005; In Final Form: June 9, 2005

On the added-row reconstructed Ag(110)(n×1)-O surfaces where one-dimensional −Ag−O−Ag−O− chains arrange periodically, the clean-off reaction of O adatoms by CO was investigated using variable temperature scanning tunneling microscopy (VT-STM). Based on the in situ STM observations of the surface structure variation in the course of the reaction at various temperatures, we found that the reaction kinetics are significantly affected by the structural transition of AgO chains from a solid straight line configuration to dynamically fluctuating configurations. Below 230 K where the chains are straight, the reaction takes place only at the end of the chains, so that the reaction progresses in the zero-order kinetics with the reaction front propagating along the chain. The temperature dependence of the reaction rates yields the activation barrier of 41 kJ/mol and the preexponential factor of 1.7×10^3 cm^{-2} s^{-1}. At room temperature, the reaction rate is drastically accelerated when almost half of the O adatoms are eliminated and the chains start fluctuating. The dynamic formation of active sites equivalent to the end of chains upon the chain fluctuation results in the nonlinear increase of the reaction rate.

1. Introduction

Most catalytic surfaces are not homogeneously reactive but often show high reactivity only at sites such as steps, kinks, and vacancies. Since Taylor[1] proposed the notion of *active sites* where reactions take place preferentially, researchers have attempted to identify the active sites and unveil the underlying mechanism of their activity. The advent of scanning tunneling microscopy (STM) has proved to be the key to unlocking the exact nature of active sites. For example, the STM study of Zambelli et al.[2] showed that the dissociation of NO on Ru(0001) occurs only at atomic step sites. According to the adsorption experiments of Dahl et al.[3] together with density functional theory calculations, the role of steps in dissociative adsorption of N_2 on Ru(0001) is to decrease the dissociation barrier by a combination of electronic and geometrical effects. In addition, recent STM works showed that some reactions occur preferentially at the peripheries of ordered arrays of adsorbates.[4−8]

The fluctuating configurations of low-dimensional structures such as steps, vacancies, and adsorbate arrays can be thermodynamically favorable at finite temperatures, because the free energy gain from the increasing entropic term overcomes the energy cost accompanied by local structural fluctuation with the increase of temperature. The step wandering and roughening transitions observed on metal surfaces are a typical manifestation of this thermodynamic principle.[9] This principle is applicable to not only low-dimensional systems at surfaces but also nanostructured materials such as clusters and macromolecules. Small metal clusters, which often act as good catalysts, have several types of structural isomers whose total energies are close to each other.[10] Therefore, conversion among the different isomers can take place at finite temperatures. Enzymatic protein molecules have a huge number of degrees of freedom, and thus they are also likely susceptible to thermal fluctuation. The structural transition from one configuration to another creates active sites dynamically, which may affect the catalytic activity of these "soft" materials. Therefore, the dynamical formation of active species and sites by structural fluctuation is a key issue in establishing a microscopic model for chemical reactions at solid surfaces and nanostructured compounds ranging from metal clusters to life-sustaining protein molecules.

The dissociative adsorption of oxygen molecules onto the (110) surfaces of face centered cubic metals often leads to the formation of one-dimensional (1D) structures, which is accompanied by mass transfer of substrate atoms. Since 1D systems are more susceptible to structural fluctuation than 2D and 3D systems, the structural fluctuation affects their reactions with small molecules arriving at surfaces covered with these 1D structures. Reactions of CO with O in such quasi-1D structures formed on Rh(110)[4] and Cu(110)[5] have been studied using STM; O atoms are highly reactive at the edges of these structures. However, these structures form rigid 2D islands due to the mutually attractive interactions, so that they are poor candidates for proving the above proposition. The −Ag−O−Ag−O− chains on Ag(110) are more promising. The AgO chains arrange periodically to form (n×1) ($n = 2-7$), depending on O fractional coverage, θ_O, due to repulsive interchain interactions.[11−13] While the chains appear as rigid straight lines in the (2×1) structure at room temperature, the structure fluctuates, resulting in segmented and sometimes frizzy chains in the (n×1) ($n > 4$) structures as schematically depicted in Figure 1.[13] Energetically equivalent structures of different segment configurations exist, reflecting the 1D nature of chains. Thus, chains fluctuate among the different configurations rather

[†] The Graduate University for Advanced Studies (Sokendai).
[⊥] Current address: Catalysis Research Centre, Hokkaido University, Sapporo 060, Japan.
[‡] Institute for Molecular Science.
[§] University of Tokyo.

10.1021/jp0512154 CCC: $30.25
Published on Web 07/12/2005

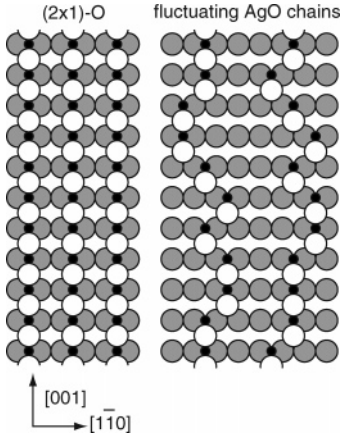

Figure 1. Schematic models of (2×1)-O structure and fluctuating AgO chains in (5×1)-O. Larger open and gray circles are surface and second-layer Ag atoms, respectively, and smaller filled circles are O atoms.

than freezing into a single configuration. Therefore, AgO chains on Ag(110) provide a good opportunity to investigate the effects of structural fluctuation on reactivity.

The oxidation of CO on O-covered metal surfaces has been extensively investigated as a prototype of catalytic reactions. This reaction proceeds with the Langmuir−Hinshelwood mechanism, in which CO arriving at the surface from the gas phase migrates on the surface, reacts with an O adatom, and then produces CO_2 that desorbs as a reaction product. Since Ag surfaces are industrially useful catalysts in the selective oxidation of ethylene to ethylene oxide, the oxidation of CO on Ag(110) has been examined using various techniques such as thermal desorption and molecular beam scattering.[14−22] The oxidation of CO on Ag(110)(2×1)-O is often called the "clean-off" reaction and O adatoms are easily removed by CO as desorbing CO_2 below 100 K.[22] However, microscopic correlation between the surface structure and the reaction kinetics has not been explored in detail.

In this paper, we report systematic studies on the clean-off reaction as a model reaction to clarify the influence of the structural fluctuation on the chemical reaction. We employed variable-temperature STM (VT-STM) to investigate (i) the temperature dependence of chain fluctuations, (ii) active sites and the reaction kinetics in the temperature range of 100−208 K, and (iii) the influence of chain fluctuation on the reaction kinetics. The fluctuation depends on the surface temperature and it is greatly reduced below 230 K. There were active sites at the ends of the chains and thus the reaction proceeds in zero-order kinetics at low temperatures where no chain fluctuation occurs. In contrast, the reaction proceeds nonlinearly with increasing the exposure of CO at room temperature and the reaction rate is accelerated at low θ_O. The acceleration of the reaction is well explained by the reaction model in which the chain fluctuation dynamically creates active sites.

2. Experimental Section

Experiments were performed in an ultrahigh vacuum chamber equipped with a VT-STM (Omicron GmbH). The base pressure was below 1×10^{-10} Torr. A clean Ag(110) surface was prepared by sputtering and annealing at 800 K. STM measurements at various temperatures between 35 K and room temperature were performed by using an electrochemically etched W tip. The sample temperatures were kept constant by controlling both the flux of liquid He and the electric power applied to the heater of the cryostat. The in situ titration measurements

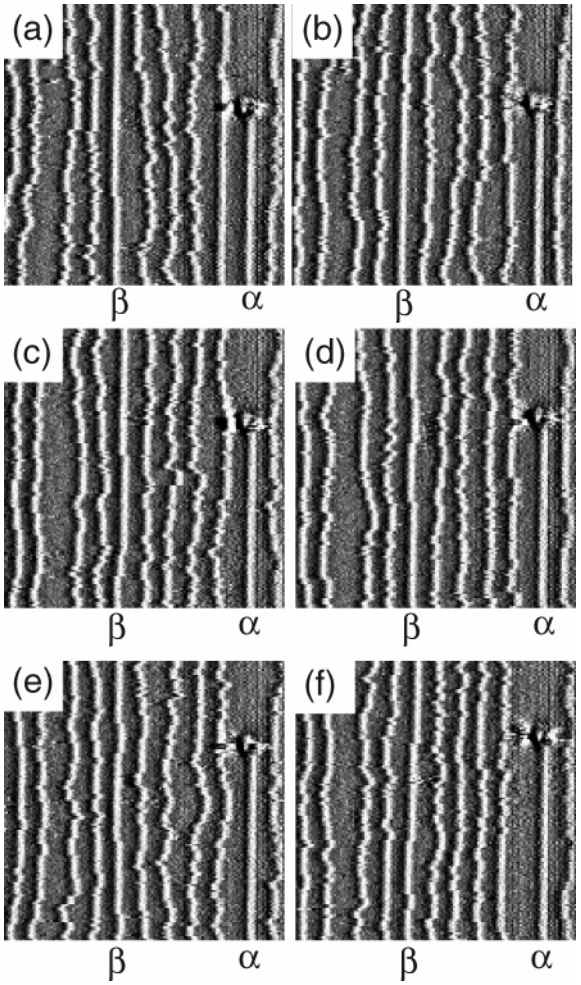

Figure 2. A series of STM images of 30 × 30 nm^2 continuously taken for the (9×1)-O surface in constant height mode at room temperature (V_{tip} = 2.0 V). The (9×1)-O surface was prepared by exposing the Ag(110) surface to 6 L of O_2 at room temperature (1 L = 1×10^{-6} Torr s). The scanning rate is 12 s per image.

of the clean-off reaction were carried out by first preparing the (n×1)-O structure (n = 2−6) and then removing O adatoms with CO. STM images of the same region were sequentially taken in the constant current mode under CO exposure. A high tunneling resistance of more than 1 GΩ was used to reduce tip−surface interactions. Typical tip bias and tunneling current used were +1 to +2.5 V and 0.1 to 0.3 nA, respectively.

3. Results and Discussion

3.1. The Structural Fluctuation of AgO Chains and the Temperature Dependence. Previous STM works have reported that AgO chains fluctuate at room temperature.[12,13] Two kinds of fluctuating chains are observed: one at low θ_O as reported by Pai et al.[13] and the other at domain boundaries between different reconstructed phases, for example, (2×1)-O and (3×1)-O.[12] The latter fluctuation is associated with the existence of energetically equivalent sites. Both types of structural fluctuation were observed in this study, but we focus on the chain fluctuation observed at low θ_O.

Figure 2 shows the consecutive STM images of fluctuating AgO chains in the (9×1)-O phase at room temperature. These images were acquired in a constant height mode at the scanning rate of 12 s per image. Almost all the chains are fluctuating. The fluctuating configurations of the chains are different from image to image, which indicates that the chains are not frozen

into one configuration but travel among various configurations. From the scanning rate, the fluctuating interval is roughly estimated to be several tens to several hundreds of milliseconds. Taking a closer look at these chains, one notices that the fluctuating motions of several pairs of neighboring chains are correlated, that is, several segments of the neighboring chains are displaced in the same direction. These motions are caused by the repulsive interactions between the chains. Interestingly, the chains denoted by α and β are much less fluctuating than the others. They appear as almost straight lines while the others bend and wind. In particular, the α chain remained straight and did not fluctuate during the observation. These less fluctuating chains show a common structural feature: the end of a chain (α) shows a protrusion possibly due to termination by impurities, or the end of a chain (β) is attached to a step edge (not shown) while the fluctuating chains have free ends (see Figure 9c,d). The similar structural features of chains with less fluctuation have been observed in the previous STM results of Pai et al.[13] They pointed out that the structural fluctuation does not occur when the end of a chain is attached to (i) impurity, (ii) the lower side of the step, and (iii) another chain in the lower or upper terrace across the step edge.

The experimental finding that the pinning of the chain at its end largely reduces fluctuation provides some insight on the fluctuation dynamics. Considering a chain as a string composed of AgO units, fluctuating configurations are formed as a result of the thermally excited displacement of each unit along the $[1\bar{1}0]$ direction. The fluctuation dynamics are governed not only by the thermodynamic balance between the competing terms in the free energy of an AgO chain but also by the activation barrier for displacement of each AgO unit. It is reasonable to assume that the barrier height for the AgO unit inside the chain with a pinned end is the same as that with free ends because the influence of the pinning seems local in nature. The structure at the free end is relaxed more extensively than that of the middle of chains, indicating that the bonding expectedly becomes loose at the free end. Thus, the activation energy for the displacement of an AgO unit along the $[1\bar{1}0]$ direction is sufficiently low at the free end. Once the AgO unit at the end is displaced, the bonding of the neighboring AgO unit weakens and then it can be displaced easily. In this way, the displacement of the AgO unit located at the end triggers the entire fluctuation motion of the chain. In contrast, the activation energy is larger at the end pinned by impurity or step, and thus the chain remains straight.

The temperature dependence of the chain fluctuation was measured for (9×1)-O and (5×1)-O surfaces by STM. Figure 3 shows STM images taken for the (9×1)-O surface at various temperatures. The STM images were observed after heating the sample from 200 K to the desired temperatures. Keeping the sample temperature constant requires about an hour. Although this elapsed time would be sufficient to equilibrate AgO chains on the surface, we could not trace the same area due to thermal drift upon changing temperatures. Thus, we measured different places with a similar chain density and a terrace size. These STM images clearly show that the structural fluctuation is reduced with the decrease of temperature. When the sample was cooled back to 200 K, the fluctuations cease so that the chains become straight. Thus, the structural change takes place reversibly. We estimated the average number of segments per chain as an order parameter by superimposing the (1×1) unit mesh on each STM image. The results are summarized in Figure 4 as a function of temperature for both (9×1)-O and (5×1)-O surfaces. They indicate that the degree of fluctuation is continuously reduced with the decrease of sample temperature,

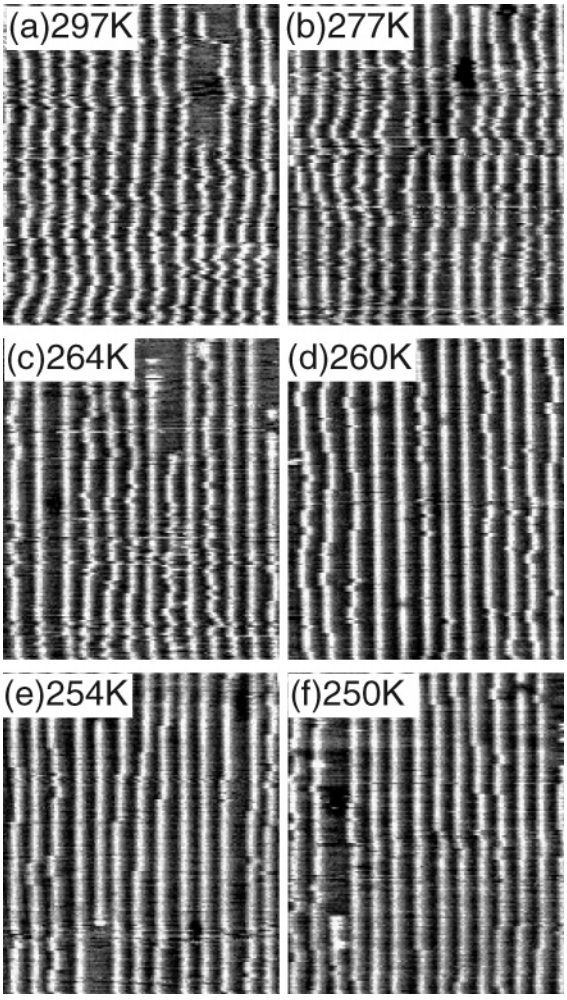

Figure 3. STM images of 25.7 × 30 nm^2 taken for the (9×1)-O surface at various temperatures from 250 K to room temperature in constant current mode (V_{tip} = 2.3 V and I_{tunnel} = 0.2 nA). The (9×1)-O surface was prepared by exposing the Ag(110) surface to 6 L of O_2 at room temperature. These images are taken for different places because of thermal drift upon the sample heating.

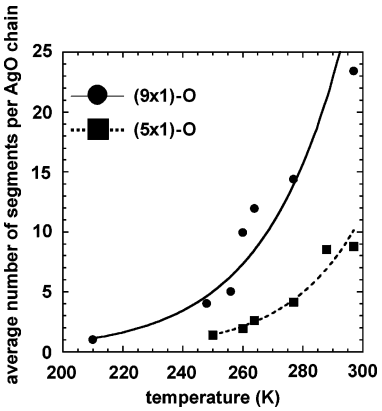

Figure 4. The temperature dependence of the average number of segments per AgO chain for (9×1)-O and (5×1)-O surfaces. The (5×1)-O was prepared by exposing the Ag(110) surface to 20 L of O_2 at room temperature. Theses values were estimated by superimposing the (1×1) mesh on each STM image of 25.7 × 30 nm^2. The lines serve as a viewing guide.

and that the chain fluctuation is frozen below 250 K for the (5×1)-O surface. The chains are frozen at the lower temperature for the (9×1)-O surface. This reflects that the repulsive interchain interactions are weaker as the distance between the chains becomes longer.

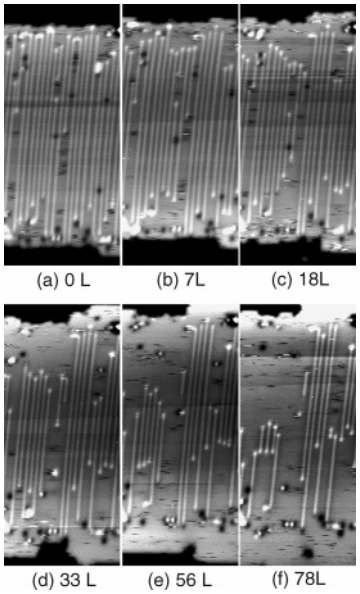

Figure 5. A series of STM images of 30 × 68 nm^2 continuously taken in the course of the clean-off reaction on the (6×1)-O surface at 195 K. These images were taken in constant current mode (V_{tip} = +1.8 V and I_{tunnel} = 0.2 nA). The CO pressure was 2.3 × 10^{-8} Torr. 1 L = 1 × 10^{-6} Torr s.

The direct interaction (i.e., electrostatic interaction and the direct overlap of electronic orbitals) and the indirect interaction through substrate mediated by lattice deformation and valence electrons are candidates as the origins of repulsive interactions between AgO chains in analogy with the adsorbate−adsorbate interactions.[23,24] Among them, the indirect interaction mediated by substrate deformation has been proposed as the origin of the repulsive interaction between Ag−O chains by Schimizu and Tsukada[25] based on the first-principles calculations for Ag(110)(n×1)-O (n = 2, 3) and Cu(110)(2×1)-O surfaces. The larger lateral displacement along the [1$\bar{1}$0] direction of the substrate atom in the second layer bonded to the added-rows was observed for the Ag(110)(2×1)-O surface. Since the sizable displacement was not observed for the Cu(110)(2×1)-O surface where the attractive interaction leads to the formation of (2×1)-O islands, it was concluded that the large displacement for the Ag(110)(2×1)-O surface raises the total energy and leads to the repulsive interaction between the chains. However, recent first-principles calculation has shown that the large lateral displacement of the substrate atoms does not take place.[26] The origin of the interchain interaction on Ag(110) surfaces is still unclear.

3.2. Active Sites and Kinetics for the Clean-Off Reaction at Low Temperatures. The sequential STM images taken in the course of the clean-off reaction demonstrate clearly where the reaction occurs and how the reaction proceeds. Figure 5 shows the surface structure variation during the clean-off reaction at 195 K on the Ag(110)(6×1)-O surface that was prepared by exposing the clean Ag(110) surface to O_2 of 15 L (1 L = 1 × 10^{-6} Torr s) at room temperature. The CO pressure was kept at 2.3 × 10^{-8} Torr. Note that the chain fluctuation is significantly reduced at 195 K so that the influence of the structural fluctuation on the reaction is negligible. Figure 5a shows the (6×1)-O surface before exposure to CO, where all the AgO chains extend from step to step. The horizontal lines seen in the upper and lower part of the STM image are steps running along the [1$\bar{1}$0] direction. The small black circles are tentatively assigned to vacancy islands. When CO gas is introduced, the reaction starts gradually. As the reaction proceeds, all the chains become shorter and finally disappear completely. No chains were observed that were broken into segments in the middle of the chain. These results indicate that the reactivity of the O adatoms at the ends of the chains is so high that the reaction occurs only at the ends of the chains. Considering the time resolution of STM, one might think that the segmented chains formed by the reaction occurring randomly at the middle of the chain rearrange to reappear as a longer straight chain during the interval of sequential STM scans. However, this can be ruled out because the motion of chains is entirely frozen at the present temperature range as discussed in Section 3.1.

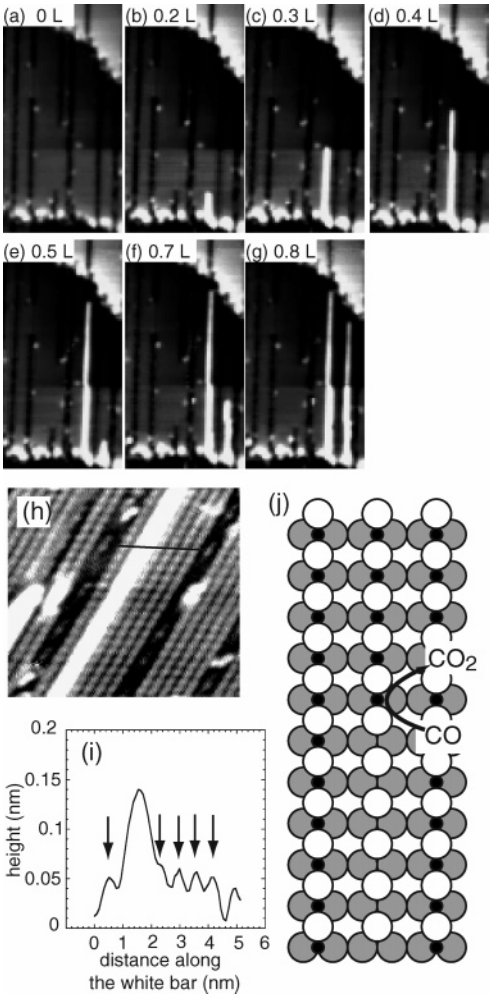

Figure 6. A series of STM images of 30 × 68 nm^2 continuously taken in the course of the clean-off reaction on the (2×1)-O surface at 100 K (a−g). Each image was acquired in constant current mode (V_{tip} = +1.4 V and I_{tunnel} = 0.2 nA). The nominal CO pressure was 5 × 10^{-10} Torr. 1 L = 1 × 10^{-6} Torr s. (h) High-resolution STM image of the brighter line structure taken in constant current mode after the surface reacted with CO at 100 K was cooled at 35 K (V_{tip} = −1.1 V, I_{tunnel} = 0.2 nA, and image size = 10 × 10 nm^2). (i) The cross-sectional profile of the bright line structure along the line as shown in part h. (j) Schematic model of the brighter line structure (larger open and gray circles are surface and second-layer Ag atoms, respectively, and smaller filled circles are O atoms).

The morphology of the step edges also changes with the removal of O adatoms. This indicates that the Ag adatoms formed on the terraces by the reaction migrate and attach to the step edges. According to the STM work about homoepitaxy on Ag(110), Ag adatoms are mobile above 180 K.[27]

The in situ STM observations were also carried out at 100 K and the results are summarized in Figure 6. The reaction starts

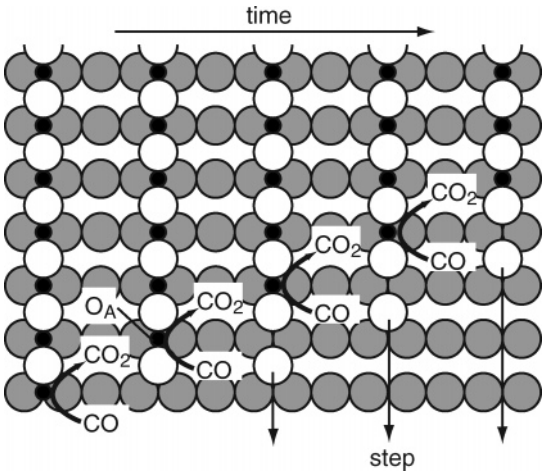

Figure 7. Schematic model of the structural variation in the AgO chain upon the clean-off reaction. Larger open and gray circles are surface and second-layer Ag atoms, respectively, and smaller filled circles are O atoms.

at the step edge [Figure 6b] and then the chain becomes gradually shorter while a brighter line structure grows as the CO exposure increases [Figures 6b−g]. Similar to the STM results acquired at 195 K, no evidence was observed that the reaction takes place in the middle of chains to break chains into shorter pieces. These results indicate that the reaction occurs only at the end of chains and the reaction front propagates along the chain.

The cross-sectional profile of the line structure and the fact that Ag adatoms are immobile on the terrace at 100 K lead us to conclude that the brighter line structure is attributed to the Ag adatoms aligned along the [001] direction which are left behind after the removal of O adatoms [Figure 6j]. The high resolution image of the 1D brighter structure is shown in Figure 6h where the unit of the (2×1)-O surface is also observed. The cross-sectional profile along the line in Figure 6h shows that the brighter 1D structure is 0.14 nm in height which is almost the same as the height of the atomic step on the Ag(110) surface (0.14 nm) [Figure 6i]. This ensures that the line structure is associated with Ag adatoms left behind from the reaction. Interestingly, this structure is about 0.1 nm higher than the AgO chains. The height of AgO chains has already been measured precisely in the structural analysis work by using low energy ion diffraction, i.e., 0.154 nm for the Ag atoms in AgO chains located in the 4-fold sites.[31] The reason the AgO chains appear much darker than the line structures is that the STM image reflects mainly not only atomic structure but also electronic structure. The density of states of AgO chains around the Fermi level is lower than that of the Ag adatoms on the same terrace.

Noticeably high reactivity at the ends of chains can be explained by differences in the bonding configurations of O in the chains. If a chain terminates with O as shown in Figure 7, this oxygen will be highly reactive because it is not sandwiched between two Ag adatoms, and is directly exposed to CO. Thus, this reacts first and the O adatom in the A site (denoted as O_A) then remains. The Ag−O bonding configuration of O_A relaxes differently from that inside the chain because the Ag atom at the end of the chain is bonded only to the O_A. This may make the O_A slightly less bound and more reactive. While Ag atoms not bonding to O can migrate on the surface above 180 K, they are frozen at 100 K. Therefore, the enhanced reactivity of O_A seems not to depend on whether the Ag atom at the end of the AgO chain has a neighboring Ag atom.

The temperature dependence of reaction rates provides us the activation barrier and preexponential factor of the reaction.

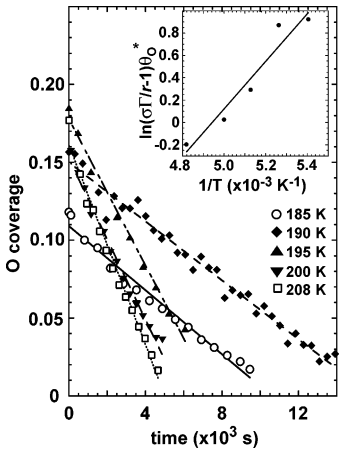

Figure 8. Time evolution of O coverage obtained by the in situ STM measurements at various temperatures from 185 to 208 K. The inset shows the Arrhenius plot of eq 7.

Titration curves taken at 185−208 K are summarized in Figure 8. Since the reaction occurs only at the ends of the chains, θ_O is decreased linearly as a function of CO exposure, i.e., the reaction follows zero-order kinetics. Generally, the following reaction mechanism on CO oxidation at the surface is accepted:

$$CO_{(g)} \xrightarrow{k_{ad}} CO_{(ad)} \quad (1)$$

$$CO_{(ad)} \xrightarrow{k_{des}} CO_{(g)} \quad (2)$$

$$CO_{(ad)} + O_{(a)} \xrightarrow{k} CO_{2(ad)} \quad (3)$$

$$CO_{2(ad)} \rightarrow CO_{2(g)} \quad (4)$$

Step 3 involves the migration of CO in weakly chemisorbed states over the surface to seek out adsorbed O atoms to react. By using the stationary state approximation for θ_{CO} combined with the fact that CO_2 desorbs soon after the formation on Ag(110), the overall reaction rate, r, is determined by steps 1−3 as follows,

$$r = -\frac{d\theta_O}{dt} = k\theta_O\theta_{CO} = \frac{k\sigma\Gamma\theta_O}{(k_{des} + k\theta_O)} \quad (5)$$

where σ is the sticking coefficient of CO, Γ is the flux of CO arriving at the surface, k_{des} is the rate constant of CO desorption, and k is the rate constant of CO oxidation. Since the reaction occurs only at the end of the chains, θ_O in the left-hand side of the eq 5 is replaced by the number of chain ends θ_O*:

$$r = -\frac{d\theta_O}{dt} = \frac{k\sigma\Gamma\theta_O*}{(k_{des} + k\theta_O*)} \quad (6)$$

Since θ_O* is almost constant as long as the number of chains does not change, the eq 6 indicates that θ_O deceases linearly over the course of the reaction as shown in Figure 8. After some algebra, eq 6 is converted into

$$\left(\frac{\sigma\Gamma}{r} - 1\right)\theta_O* = \frac{\nu_{des}}{\nu}\exp\left\{-\frac{(E_{des} - E)}{RT}\right\} \quad (7)$$

where E (E_{des}) and ν (ν_{des}) are the activation barrier and the preexponential factor of the CO oxidation (CO desorption), respectively. The Arrhenius plot of $\ln(\sigma\Gamma/r - 1)\theta_O^*$ as a function of $1/T$ gives the apparent activation barrier, $E_{des} - E$, as the slope, and the apparent preexponential factor, ν_{des}/ν, as the

intercept at $1/T = 0$ as shown in the inset of Figure 8. According to the kinetics study on CO desorption from Ag(110) of Burghaus et al.,[20] the preexponential factor and the activation barrier are $\nu_{des} = 4 \times 10^{13}$ s^{-1} and $E_{des} = 23$ kJ/mol, respectively. Using these values with $\sigma = 1$ and $\Gamma = 0.01$ ML s^{-1} (1 ML $= 8.45 \times 10^{14}$ cm^{-2}), the activation barrier of $E =$ 41 kJ/mol and preexponential factor of $\nu = 1.7 \times 10^3$ cm^{-2} s^{-1} are obtained. Typical activation barriers for CO oxidation on metal surfaces range from 40 to 100 kJ/mol.[28] The present value is close to the lower limit of this energy range, indicating that the reaction occurs even below 100 K. For bimolecular surface reactions which take place according to the Langmuir−Hinshelwood mechanism, $\nu_r = 10^{-4}-10^4$ cm^2 s^{-1} is roughly estimated by the transition state theory.[29,30] The present value reasonably agreed with this estimation. The preexponential factor is proportional to $Q_{com}/Q_{CO}Q_O$, where Q_{com}, Q_{CO}, and Q_O are the partition functions of an activated complex, adsorbed CO, and O adatom, respectively. The large preexponential factor may reflect that the reaction occurs only at the ends of the chains where the spatially less-constrained configuration of the transition state increases the degrees of freedom.

The Arrhenius parameters for the CO oxidation on Ag(110) have been obtained by other research groups. Bowker et al.[16] have measured the reaction rate in the temperature range from 150 to 400 K by monitoring the partial pressure of produced CO_2 during CO exposure. They estimated the activation energy and the preexponential factor to be $E = 22$ kJ/mol and $\nu = 3 \times 10^{-3}$ cm^{-2} s^{-1}, respectively. Burghaus and Conrad[21] have investigated the CO oxidation by using reactive molecular scattering, and have reported $E = 18$ kJ/mol and $\nu = 0.3$ cm^{-2} s^{-1} which were corrected recently as $E = 12$ kJ/mol and $\nu = 1 \times 10^3$ cm^{-2} s^{-1}. The reaction rates measured in these works follow normal kinetics in contrast to our results and the activation energies are smaller than that estimated in the present work.

Although the discrepancies are not clear in the present stage, we speculate that the previous results may suffer from impurities at the surface. Carbon impurities are difficult to remove and the clean-off reaction is very sensitive to those as clearly shown in our previous works.[7,32] A small number density of carbon atoms at the surface gives rise to bundling of AgO chains and reduces fluctuation motions of the chains even at low θ_O and thus affects the reaction kinetics. In addition, the measurements of Bowker et al. were made in a wide temperature range where the chain fluctuation affects the reaction kinetics significantly. Therefore, the kinetic parameters should be revised by the reaction model appropriate to the experimental conditions. The larger activation energy estimated in this work may be rationalized in the following way. The theoretical work of Zhang and Hu[33] points out that the activation energy of CO oxidation can be described as $E = E_O + E_{CO} + E_{surf} + E_m$, where E_O (E_{CO}) is the energy required to activate an adsorbed O (CO) to the transition state, E_{surf} is the energy associated with the surface relaxation upon the reaction, and E_m is a mixing term that includes the O−CO bond formation energy and energy due to bonding competition. Since E_{CO} and E_{surf} are usually small, E_O is the main contributor to E. We can roughly estimate E_O by taking into consideration that the diffusion of O is similar to the activation process. The diffusion barriers of O on various metal surfaces range from 50 to 100 kJ/mol,[34] which amount to 10−30% of the chemisorption energies for O adatoms. Although the diffusion barrier for O on Ag(110) has not been reported yet, it is estimated to be 30−40 kJ/mol from the chemisorption energy of 320−340 kJ/mol for O on Ag(110).[35]

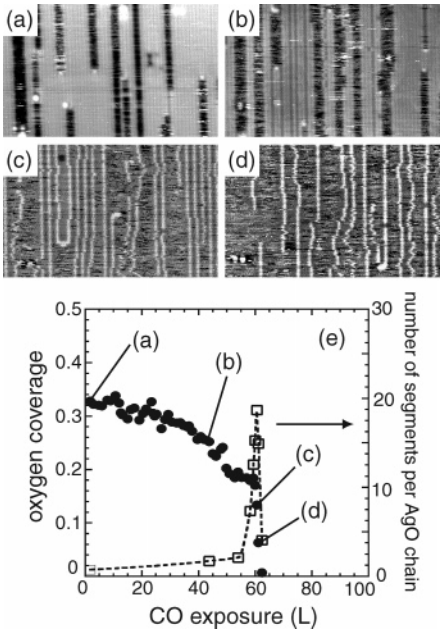

Figure 9. A series of STM images of 37×27 nm^2 continuously taken at room temperature under a nominal CO pressure of 1×10^{-8} Torr for (2×1)-O surface (a−d) ($V_{tip} = +1.4$ V and $I_{tunnel} = 0.2$ nA). (e) Time evolution of θ_O obtained for the (2×1)-O surface (filled circles). The relative number of segments for the (2×1)-O surface is also plotted (open squares). The dashed curve is drawn as a viewing guide.

This estimation is not unreasonable considering that the diffusion barrier for O_2 on Ag(110) is 21 kJ/mol.[36] Thus, including the other energy terms may explain our estimated activation energy. However, since the above discussion involves a few assumptions, further experimental and theoretical efforts are desired to clarify the above discrepancies.

3.3. Kinetics of the Clean-Off Reaction at Room Temperature and the Role of Chain Fluctuation. The in situ STM observations conducted at room temperature show markedly different kinetics compared with those observed at low temperatures. The STM observations during the clean-off reaction were made. The (2×1)-O structure was prepared at first and then exposed to CO. Figure 9 summarizes the STM images and the titration curve. The (2×1)-O phase prepared on the Ag(110) surface changes to (4×1) and (6×1) structures as the reaction progresses [Figure 9b−d]. This is a reversal in the structural change compared with the adsorption of O. Note that AgO chains in the (6×1)-O structure were observed to bend and fluctuate. The titration curve indicates that the reaction proceeds in a strongly nonlinear fashion: initially, the reaction proceeds gradually, but accelerates suddenly at $\theta_O \sim 0.2$ where the fluctuating chains appear [Figure 9e]. A similar change in the reaction rate has been observed previously.[14,15,17] Combined with the finding by the STM observations at low temperatures that the ends of chains are active sites, the strong nonlinearity observed at room temperature is explained by the following reaction model: Initially, the reaction occurs at the chain ends and proceeds one-dimensionally along the chains. As θ_O decreases, the chains are rearranged in parallel with the reaction, so that the surface structure changes from (2×1)-O to (n×1)-O ($n > 3$). As the interchain separation becomes wider, the chains become more segmented. Since O adatoms at the ends of segments are reactive, the segmentation of chains enhances the number of active O adatoms to react with CO. As a result, the reaction accelerates as θ_O decreases.

This scheme can be reinforced by comparing the variation in the number of segments over the course of the reaction with

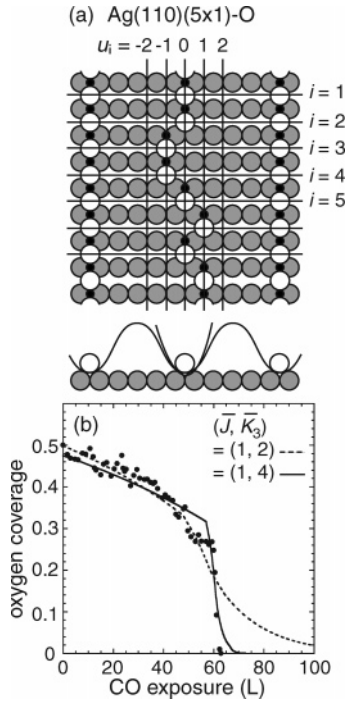

Figure 10. (a) Schematic of a fluctuating chain. The displacement of the *i*th AgO unit, u_i, is shown graphically. The model potential is illustrated by the approximated parabola. (b) Comparison of experimental (filled circles) and theoretical titration curves calculated for $(\bar{J},\bar{K}_3) = (1,2)$ and (1,4) (dashed and solid curves). Experimental results are corrected so that the initial θ_O is 0.5 for comparison.

the titration curves. The relative number of segments can be evaluated by superimposing a mesh consisting of (2×1) unit cells onto the STM images. The peak position of the number of segments coincides with the sudden drop in the titration curve as shown in Figure 9e. The reaction rate is proportional to θ_O* and thus increases drastically.

Quantitative features regarding the fluctuation of chains and θ_O* can be obtained using the Ising model,[7] which was originally proposed by Sasaki et al.[37] Fluctuation is assumed to occur in a thermal equilibrium. Although the chain shape and θ_O* are time-dependent, the average chain length in thermal equilibrium is calculated and then θ_O* is estimated. It is reasonable to assume that the titration curve measured under the present experimental conditions (200 s/image) samples an ensemble average of θ_O* over the thermal distribution of fluctuating chains rather than an instantaneous value of a fluctuating chain.

An AgO chain is first defined as a string of AgO units moving across the (1×1) lattice points only in the $[1\bar{1}0]$ direction. With the displacement of the *i*th AgO unit, u_i, defined as shown in Figure 10a, each fluctuating chain is then described by a set of u_i. The value of u_i is restricted to vary from $-(n-1)/2$ to $(n-1)/2$ for the (*n*×1)-O structure; this prohibits collision between the AgO units of the nearest neighbor chains. The calculation was performed only for odd *n* because its symmetry simplifies the calculation. Each AgO unit feels attractive intrachain and repulsive interchain interactions, as mentioned earlier. The nearest neighbor interaction energy, $W(u_i,u_{i+1})$, and the potential energy, $V(u_i)$, are then treated as intra- and interchain interaction energies, respectively. Thus, the total energy of a chain in the (*n*×1)-O structure, $E_{total}(n)$, is given by

$$E_{total}(n) = \sum\left\{W(u_i,u_{i+1}) + \frac{1}{2}(V(u_i) + V(u_{i+1}))\right\}$$

The energy $W(u_i,u_{i+1})$ depends on the difference in the displacement of nearest neighboring units as

$$W(u_i,u_{i+1}) = 0, |u_i - u_{i+1}| = 0$$

and

$$W(u_i,u_{i+1}) = J, |u_i - u_{i+1}| = 1$$

where J is the excitation energy needed to create the configuration with $|u_i - u_{i+1}| = 1$. Since the STM images reveal no AgO segments in the fluctuating chains displaced by $|u_i - u_{i+1}| > 1$, $W(u_i,u_{i+1})$ is taken as infinity for $|u_i - u_{i+1}| > 1$. For the potential energy $V(u_i)$, a mean-field model potential is assumed as follows:

$$V_n(x) = V_0(1 - \cos((2\pi/n))x)/2$$

which ensures that the (*n*×1)-O structure is most stable. This model potential is further expanded around the minimum

$$V_n(u_i) = K_n u_i^2$$

where $K_n = V_0/4(2\pi/n)^2$ as shown in Figure 10a. Note that K_n values ($n > 3$) are automatically determined once K_3 is specified.

Using the transfer matrix technique,[38] the distribution of displacements and average length of segments displaced by u can be estimated and thus θ_O* is evaluated for each (*n*×1)-O structure as a function of $(\bar{J},\bar{K}_3) = (J/k_BT, K_3/k_BT)$, where k_B is the Boltzmann constant. The comparison between the experimental and simulated titration curves is made in Figure 10b. The experimental results are reproduced reasonably well for $(\bar{J},\bar{K}_3) = (1,4)$. The value of $\bar{J}$ is consistent with the work of Sasaki et al., in which $\bar{J}$ of 1.5 is used. Thus, at $T = 300$ K, J and V_0 are estimated to be ~25 and ~100 meV, respectively, which implies that the AgO chains fluctuate easily at room temperature, as observed by STM.

The Ag−O bonding is basically characterized by three pairs of bonding/antibonding states formed by the hybridization of O 2p orbitals with Ag 4d bands. There are two occupied antibonding states below the Fermi level, E_F, and one partially occupied antibonding state crossing E_F.[39,40] Thus, electron filling of antibonding states is the origin of the small value of J. This qualitative explanation is reinforced by comparison of the electronic structure and flexibility of the 1D chains between Ag(110)(2×1)-O and Cu(110)(2×1)-O. Although two antibonding states are fully occupied in Cu(110)(2×1)-O similar to those in Ag(110)(2×1)-O, one antibonding state is located above E_F.[41] As a result, 1D Cu−O chains appear as rigid straight lines, and do not bend or fluctuate during the clean-off reaction with CO.[5] The clearly different behavior of added-row chains on both Ag(110) and Cu(110) surfaces stems from the different populations of electrons in the antibonding states.

4. Summary

We systematically measured the structural changes in AgO chains and the effect of the structural fluctuation on the clean-off reaction on Ag(110)(2×1)-O by using VT-STM. The main results are as follows: (1) The degree of chain fluctuation is reduced continuously with the decrease of temperature and is frozen below 230 K. Because of the repulsive interactions between the chains, the distribution of the displacement of AgO unit is broader as the interchain distance becomes wider. (2) Both ends of AgO chains show high reaction activity, so that the clean-off reaction at 100−208 K follows zero-order kinetics.

(3) The dynamical formation of active O adatoms in the fluctuating AgO chains at room temperature accelerates the reaction rate in a strong nonlinear fashion in $\theta_O < 0.2$ ML. The enhancement of reaction rates by the dynamical formation of active sites by thermal fluctuation should be common to chemical reactions on heterogeneous catalysts and nanostructured compounds. The current study on the quasi-1D system clearly demonstrates evidence of the influence of thermal fluctuations on reaction rates.

Acknowledgment. This work was supported in part by Grants-in-Aid for Young Scientists (A)(14703009), Scientific Research on Priority Area (417), Creative Scientific Research Collaboratory on Electron Correlation-Toward a New Research Network between Physics and Chemistry (13NP0201) from the Ministry of Education, Culture, Sports, Science and Technology (MEXT) of Japan, KAKENHI (14340176) from the Japan Society for the Promotion of Science (JSPS), and the 2002-year Joint Research Project (Soken/K02-1) of Sokendai.

References and Notes

(1) Taylor, H. S. *Chem. Rev.* **1931**, *9*, 1.
(2) Zambelli, T.; Wintterlin, J.; Trost, J.; Ertl, G. *Science* **1996**, *273*, 1688.
(3) Dahl, S.; Egeberg, R. C.; Larsen, H.; Chorkendorff, I.; Törnqvist, E.; Nørskov, J. K. *Phys. Rev. Lett.* **1999**, *83*, 1814.
(4) Leibsle, F. M.; Murray, P. W.; Francis, S. M.; Thornton, G.; Bowker, M. *Nature* (*London*) **1993**, *363*, 706.
(5) Crew, W. W.; Madix, R. J. *Surf. Sci.* **1996**, *349*, 275.
(6) Wintterlin, J.; Völkening, S.; Janssens, T. V.; Zambelli, T.; Ertl, G. *Science* **1997**, *278*, 1931.
(7) Nakagoe, O.; Watanabe, K.; Takagi, N.; Matsumoto, Y. *Phys. Rev. Lett.* **2003**, *90*, 226105.
(8) Guo, X.-C.; Madix, R. J. *J. Phys. Chem. B* **2003**, *107*, 3105.
(9) Pimpinelli, A.; Villain, J. *Physics of Crystal Growth*; Cambridge University Press: Cambridge, UK, 1998.
(10) Michaelian, K.; Rendón, N.; Garzón, I. L. *Phys. Rev. B* **1999**, *60*, 2000.
(11) Engelhardt, H. A.; Menzel, D. *Surf. Sci.* **1976**, *57*, 591.
(12) Taniguchi, M.; Tanaka, K.; Hashizume, T.; Sakurai, T. *Surf. Sci.* **1992**, *262*, L123.
(13) Pai, W. W.; Reutt-Robey, J. E. *Phys. Rev. B* **1996**, *53*, 15997.
(14) Engelhardt, H. A.; Bradshow, A. M.; Menzel, D. *Surf. Sci.* **1973**, *40*, 4.
(15) Albers, H.; Van Der Wal, W. J. J.; Gijzeman, O. L. J.; Bootsma, G. A. *Surf. Sci.* **1978**, *77*, 1.
(16) Bowker, M.; Barteau, M. A.; Madix, R. J. *Surf. Sci.* **1980**, *92*, 528.
(17) Backx, C.; De Groot, C. P. M.; Biloen, P.; Sachtler, W. M. H. *Surf. Sci.* **1983**, *128*, 81.
(18) Campbell, C. T.; Paffett, M. T. *Surf. Sci.* **1984**, *143*, 517.
(19) Burghaus, U.; Conrad, H. *Surf. Sci.* **1997**, *370*, 17.
(20) Burghaus, U.; Conrad, H. *Surf. Sci.* **1995**, *338*, L869.
(21) Burghaus, U.; Conrad, H. *Surf. Rev. Lett.* **2003**, *10*, 39.
(22) Ohta, M.; Watanabe, K.; Matsumoto, Y. *J. Phys. Chem B* **2001**, *105*, 8170.
(23) White, J. M.; Akhter, S. *CRC Rev.* **1988**, *14*, 131.
(24) Nørskov, J. K. In *The Chemical Physics of Solid Surfaces*; King, D. A., Woodruff, D. P., Eds.; Elsevier: Amsterdam, The Netherlands, 1993; Vol. 6, p 1.
(25) Schimizu, T.; Tsukada, M. *Surf. Sci. Lett.* **1993**, *295*, L1071.
(26) Katagiri, H.; Uda T.; Terakura, K. *Surf. Sci.* **1999**, *424*, 332.
(27) Morgenstern, K.; Lægsgaard, E.; Stensgaard, I.; Besenbacher, F.; Böhringer, M.; Schneider, W. D.; Berndt, R.; Mauri, F.; De Vita, A.; Car, R. *Appl. Phys. A* **1999**, *69*, 559.
(28) Eichler, A. *Surf. Sci.* **2002**, *498*, 314.
(29) Zhdanov, V. P. *Surf. Sci. Rep.* **1991**, *12*, 183.
(30) Zhdanov, V. P. *Elementary physicochemical processes on solid surfaces*; Plenum Press: New York, 1991.
(31) Canepa, M.; Cantini, P.; Fossa, F.; Mattera, L.; Terreni, S. *Phys. Rev. B* **1993**, *47*, 15823.
(32) Nakagoe, O.; Ohta, M.; Watanabe, K.; Takagi, N.; Matsumoto, Y. *Surf. Sci.* **2003**, *528*, 144.
(33) Zhang, C. J.; Hu, P. *J. Am. Chem. Soc.* **2001**, *123*, 1166.
(34) Barth, J. V. *Surf. Sci. Rep.* **2000**, *40*, 75.
(35) This was estimated from 142 to 188 kJ/mol for the desorption energy of O as O_2 (ref 16) and 497 kJ/mol for the dissociation enthalpy of O_2 in the gas phase (Atkins, P. W. *Physical Chemistry*; Oxford University Press: Oxford, UK, 1982).
(36) Barth, J. V.; Zambellli, T.; Winterlin, J.; Schuster, R.; Ertl, G. *Phys. Rev. B* **1997**, *55*, 12902.
(37) Sasaki, K.; Suzuki, H.; Tanaka, K.; Okawa, Y. *Surf. Sci.* **1995**, *327*, 33.
(38) Hill, T. L. *Statistical Mechanics*; Dover: New York, 1987.
(39) Tjeng, L. H.; Meinders, M. B. J.; Sawatzky, G. A. *Surf. Sci.* **1990**, *236*, 341.
(40) Courths, R.; Hüfner, S.; Kemkes, P.; Wiesen, G. *Surf. Sci.* **1997**, *376*, 43.
(41) Courths, R. *Solid State Commun.* **1987**, *63*, 619.